Tracking Crop Phenology across different Sentinel-1 Orbits by Combining PolSAR Features with Growing Degree Data

JOHANNES LÖW[1], STEVEN HILL[2], MICHAEL THIEL[2], TOBIAS ULLMANN[2] & CHRISTOPHER CONRAD[1]

Abstract: This study harnesses Sentinel-1 time series of Alpha, Entropy, VV and VH backscatter intensities as well as their cross ratio to monitor phenological development in wheat, sugar beet, canola, and potatoes in Demmin (Germany) for the years 2017 to 2021 Overcoming challenges ranging from separate viewing geometries (incidence angles respectively) to different parametrizations of a smoothing algorithm, the assimilation of Growing Degree Days is introduced to enhance tracking capabilities. Time series analysis explores changes in crop and orbit-specific signals, addressing systematic offsets and the tracking reliability of polarimetric Sentinel-1 features. The study extends insights to canola, sugar beet, and potatoes, revealing common patterns at landscape level. Establishing a repository of remotely sensed phenological events, this research facilitates comparative analyses, enhancing crop monitoring and climate resilience assessment.

1 Introduction

In recent years, the Essential Variables (EV) concept has emerged as a tool to assess progress towards Sustainable Development Goals across policy domains (REYERS et al. 2017). GEO-GLAM currently defines key agricultural EVs, with a focus on phenology, particularly the current crop stage (GILLIAMS et al. n.d.). Phenology, crucial for crop management, provides vital information related to plant productivity and growth, especially during specific stages of the crop life cycle that are highly susceptible to meteorological conditions (GAO & ZHANG 2021; SAKAMOTO et al. 2013). Given the increasing frequency of extreme weather events and the complexities of climate adaptation and resilience, there is a growing demand for this information (Shorachi et al. 2022). Earth observation data, particularly Radar data, has been extensively studied in agriculture as a potential information source (STEELE-DUNNE et al. 2017). The launch of Sentinel-1 A&B has notably increased research interest in Synthetic Aperture Radar (SAR) data (NASRALLAH et al., 2019; PASTERNAK & PAWŁUSZEK-FILIPIAK 2023). In tracking crop phenology, three main analytical approaches have been established: (i) classifiers like Random Forest or deep learning (LOBERT et al. 2023; MERCIER et al. 2020), (ii) stochastic or statistical modeling (Canisius et al. 2018), and (iii) time series metrics (TSM)(KHABBAZAN et al. 2019; LÖW et al. 2021). This study specifically focuses on TSM in form of extreme value and breakpoint analyses. To describe plant growth, the BBCH-scale, which categorizes plant growth into micro and macro stages, is employed in this study. The terms "events" and "stages" are used interchangeably, without distinguishing between macro and micro stages. However, when a development is associated with a specific BBCH value, it is referred to as such.

[1] Department of Geoecology, University Halle-Wittenberg, Von-Seckendorff-Platz-4, D-06120 Halle (Saale), E-Mail: [Johannes.Loew, Christopher.Conrad]@geooeko.uni-halle.de
[2] Earth Observation Research Cluster University of Wuerzburg, John-Skilton-Str. 4a D-97074 Würzburg, E-Mail: [Steven.Hill, Michael.Thiel, Tobias.Ullmann]@uni-wuerzburg.de

This study tracks the phenological development of diverse crops, namely wheat, sugar beet, canola, and potatoes, providing a more comprehensive understanding compared to studies focusing on specific crops or families (HARFENMEISTER et al. 2021; SCHLUND & ERASMI 2020). Addressing the challenge posed by HARFENMEISTER et al. (2021), who emphasized the unreliable use of chronological occurrence of TSM for phenological allocation, we introduced agrometeorological data, specifically Growing Degree Days (GDD) (MCMASTER & WILHELM 1997), as a baseline to enhance phenological tracking. The mission-ending malfunction of S1B introduced a new aspect, necessitating the integration of multiple orbits to maintain a comparatively dense time series due to the loss of the six-day repetition rate.
As of January 2022, reliance on the S1 twin constellation's six-day repetition rate is no longer feasible. Consequently, we utilized archived data to concurrently track phenological development across different orbits, examining potential differences in their response, i.e. due to different viewing geometries and different incidence angles. The current assumption is that differences become negligible once a certain biomass volume is present (MERCIER et al. 2020). While previous studies addressed this question over wheat fields and sunflower plantations, they either focused on deriving biophysical parameters or exclusively investigated backscatter (ARIAS et al. 2022; QADIR et al. 2023), but not to phenology. To address these research gaps, the study poses the following questions:

- What are the major changes within a crop and orbit-specific signal during the growing season, and how are they linked to the plant's phenological development?
- How reliably can these changes be tracked across multiple growing seasons?
- Is there a recurring offset between plant changes and signal changes, and is it associated with orbit-specific viewing geometries?

2 Materials and Methods

2.1 Study area and data

The study area, situated in northeastern Germany in Mecklenburg-West Pomerania, experiences a temperate Middle-European climate with an average annual precipitation of 550 mm, perennial humidity, and a mean air temperature of 8.3 °C. Established in 2001 by the German Aerospace Center (DLR) as an Earth observation calibration site, DEMMIN is part of TERENO since 2008 and a member of JECAM since 2018 (SPENGLER et al. 2018).
Crop and parcel data in DEMMIN were extracted from the German integrated administration and control system (InVeKoS) for 2017-2021, focusing on wheat, sugar beet, canola, and potatoes. The study disregards distinctions between starchy and non-starchy potatoes as non-critical for phenological analysis. Field selection prioritized relevant sizes (3 ha for wheat, canola, sugar beet; 2 ha for potatoes) to minimize pixel contamination (LOBERT et al. 2023).
In situ phenological observations were obtained from the German Weather Service's (DWD) observer framework. Due to limited DWD coverage, average occurrence date at the state-level serves as the primary validation layer. This dataset also provides deviation from the mean observation date, offering a site-specific perspective on phenological progress. Recorded DWD phenological events were translated to the BBCH scale for comparability with other studies. Fig. 1 shows the area of interest as well as the coverage by the modified Invekos data.

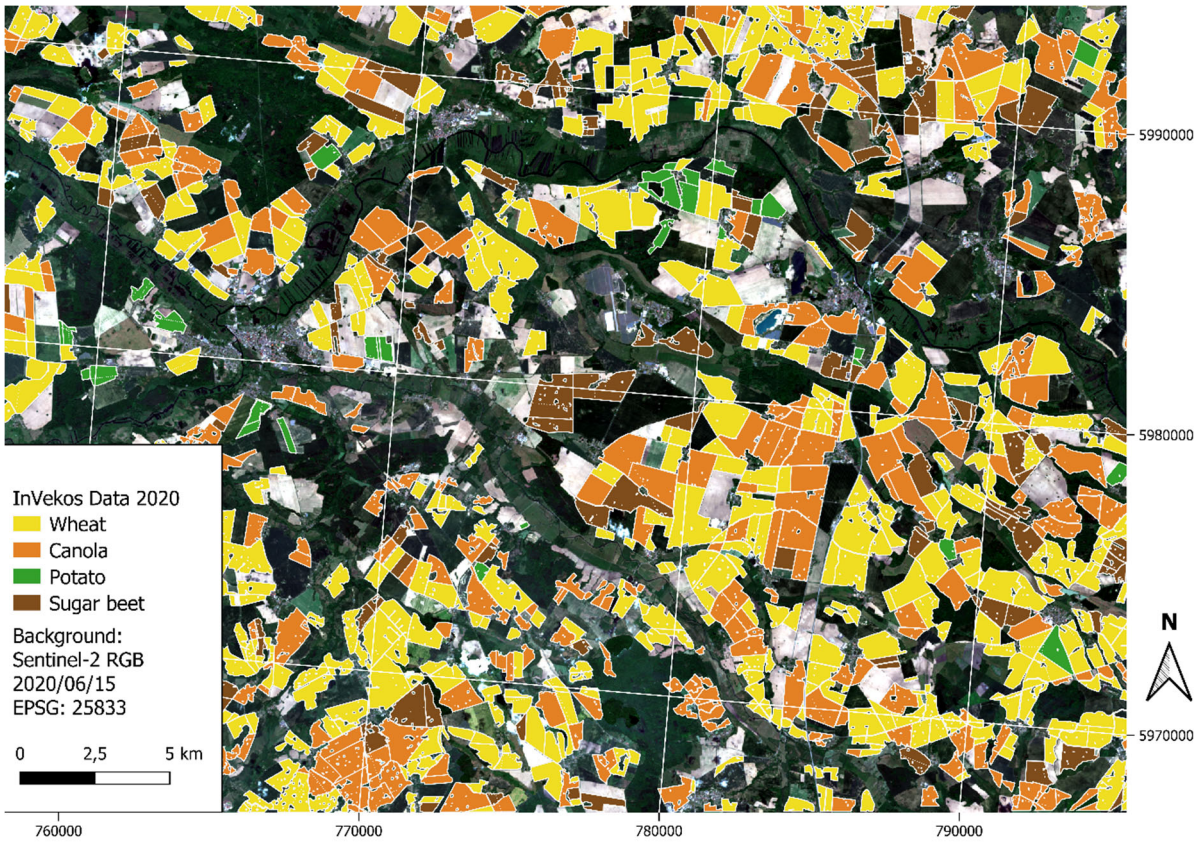

Fig 1: Study area of Demmin with Invekos data of targeted crops

2.2 Growing degree and Sentinel-1 data

GDD are heat units commonly employed to characterize the progression of biological processes (McMaster & Wilhelm 1997). They represent the accumulation of these units and serve as a widely used tool for simulating crop growth. The fundamental interpretation of this concept is computed as follows:

$$GDD = \left[\frac{(T_{max} + T_{min})}{2}\right] - T_{base}$$

Equation 1: Simple form of calculating growing degree

The equation 1 employs Tmax for daily maximum air temperature, T_{min} for daily minimum air temperature, and T_{base} for the temperature below which no plant growth occurs (McMaster & Wilhelm 1997). Widely used to translate crop phenology into crop maturity for yield models (McNairn et al. 2018), it has faced criticism for its linear nature, particularly in extreme and variable weather conditions (Ritchie & Nesmith 2015; Stinner et al. 1974). To address these concerns, a more sophisticated method proposed by Zhou & Wang (2018) is adopted. Given our observation period with extreme drought in Germany (Schlund & Erasmi 2020), this method calculates an hourly temperature time with three parameters: T_u for the upper temperature limit, Topt for optimal temperature where maximum growth occurs, and T_b for the base temperature (Zhou & Wang 2018).

$$HTT = \begin{cases} 0, & T_h < T_b \\ \left[\frac{T_h - T_b}{T_{opt} - T_b}\right]\left[\frac{T_u - T_h}{T_u - T_{opt}}\right]^{\frac{T_u - T_{opt}}{T_{opt} - T_b}} & | \; T_b \leq T_h \leq T_u \\ 0, & T_u < T_h \end{cases}$$

Equation 2: Sophisticated form of calculating growing degree

DWD provides air temperature data for the 2017-2021 observation period, interpolated from DEMMIN's network with a native spatial resolution of 500 × 500 meters per pixel and a temporal resolution of one hour, using ordinary kriging (HAßELBUSCH & LUCAS-MOFAT 2021). The GDD are aggregated as the daily mean of Heat Time Threshold (HTT) based on this dataset, serving as the second layer of validation in combination with in-situ observations recorded by DWD. These calculations, defining phenological stages as x plus or minus y GDD, are performed on the open data cube platform (ODC) using Python. Table 1 details temperature thresholds by crop type, derived from literature included in Table 1.

Tab 1: Specifications of thresholds of air temperature for calculating GDD

Crop type	T_{base}	T_{opt}	T_U	references
wheat	0	21	31	(JACOTT & BODEN 2020; MCMASTER & SMIKA 1988)
canola	4	25	34	(DERAKHSHAN et al. 2018)
sugar beet	7	24	32	(RADKE & BAUER 1969; TERRY 1968)
potato	5	22	30	(HAVERKORT & VERHAGEN 2008; RYKACZEWSKA 2015)

The S1 data time series spans relative orbits 146, 95, and 168 from 2017 to 2021, totalling about 1050 images. Acquired in Interferometric Wide Swath mode with VV/VH polarization, Single Look Complex (SLC) was chosen for polarimetric feature calculation and decomposition. The respective incidence angles and flight directions are listed in Table 2.

Tab 2: Overview of relative orbits, their flight direction and range of incidence angles

Orbit ID	Flight direction	Min. angle [°]	Max. angle [°]
146	ascending	30	41
168	descending	30	41
95	descending	41	45

PyroSAR (TRUCKENBRODT et al. 2019) and SNAP (Version 9) were used for pre-processing within an ODC environment. The processing chain included terrain flattening, multi-looking (one look in azimuth and four looks in range), speckle filtering with a 5x5 boxcar filter, and Range-Doppler Terrain correction, resulting in a 20m x 20m spatial resolution and gamma nought (GN) backscatter. Cross-pol (CR) ratio (VV-VH) was calculated, and Alpha (ALP) and Entropy (ENT) were derived from a C-2 Matrix (CLOUDE & POTTIER 1996). SRTM data (1 Arc-second) served as the digital elevation model. This set of S1 features, including VV/VH backscatter, CR, ALP, and ENT has been proven in various studies to accurately reflect changes in plant physiognomy throughout the crop life cycle (LÖW et al. 2021; SCHLUND & ERASMI 2020; VREUGDENHIL et al. 2018).

2.3 Multi orbit time series analysis

This study integrates two spatial scales: the field level and a higher level, such as a landscape, region, or any other artificial or natural stratum. In this particular investigation, the higher level (landscape level) corresponds to the extent of the DEMMIN test site.

2.3.1 Time series generation at field level

This study addresses the challenge posed by variations in smoothing algorithms and parameterization when monitoring phenological development using TSM such as break points (VERBESSELT et al. 2012; VERBESSELT et al. 2010) and extrema. To overcome this issue, the study assumes that major changes induced by phenology in crop SAR signatures remain consistent across multiple parameterizations of a smoothing algorithm. This assumption is supported by the comparison of results between SCHLUND & ERASMI (2020) and LÖW et al. (2021), who employed the same smoothing technique with different parameterizations to track common and different stages of winter wheat. To test this assumption, the study uses locally weighted scatterplot smoothing with tri-cubic weight and one-degree polynomial regression (LOESS) (CLEVELAND 1979), iterating the smoothing degree (span) from 0.05 to 0.5 in increments of 0.05 for each field. This span range covers scenarios from close to raw data (0.05) to strongly oversmoothed (0.5). Subsequently, histograms with a bin size of six days (matching the S1 revisit rate) are generated for extrema and break point occurrences at the field level. Fig. 2 illustrates this part of the framework, comparing two different acquisition geometries and exploring year-to-year variations within the same acquisition geometry.

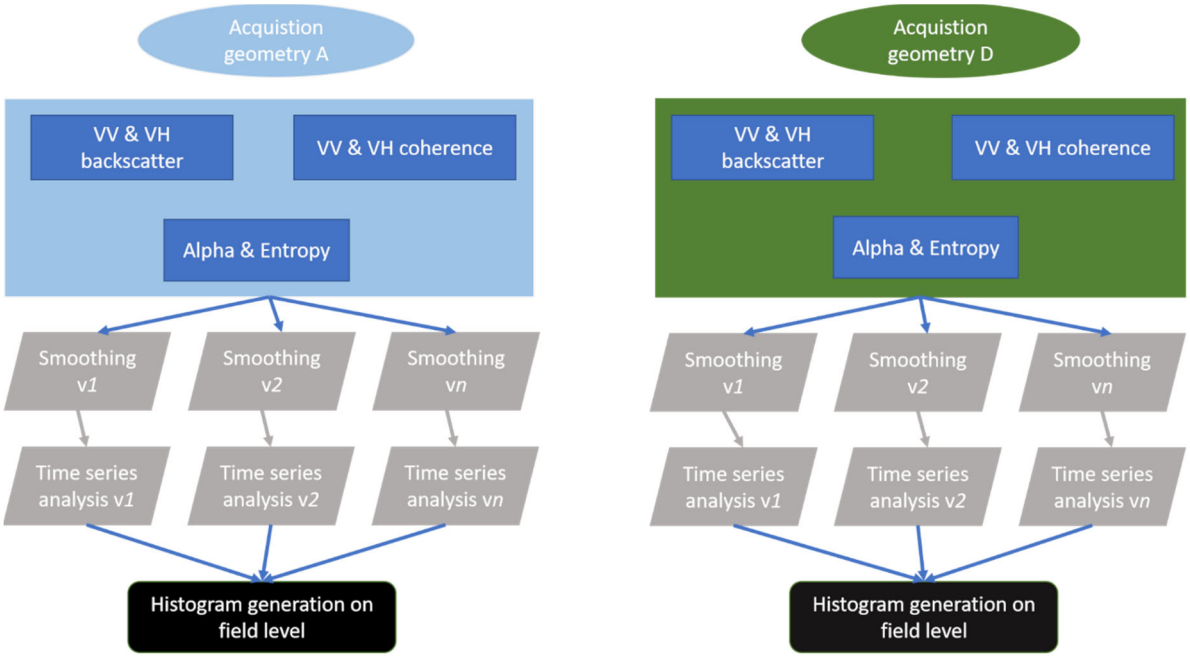

Fig 2: Generation of field-based histograms for each S1 feature containing the distribution of TSM across all-time series generated by differently parametrized LOESS smoothing

Separate histograms are created for extrema, distinguishing between minima and maxima, and additionally without the differentiation between those two types. The latter approach may indicate absence-based tracking, focusing on phases characterized by the lack of detectable changes observed through extrema.

2.3.2 Pattern extraction and tracking of phenological stages

Following the field-level analysis, histograms are generated at the landscape level for each crop type to visualize the overall distribution in the targeted area. Focusing on significant occurrences, a percentile-based approach is adopted. For extrema, the threshold is set at 0.9, equivalent to a significance level of 0.1. However, after examining histograms at a threshold of 0.9, the threshold for break points is adjusted to 0.8 to avoid underestimating the relevant number of occurrences. Fig. 3 illustrates the overall framework of the landscape-level analysis.

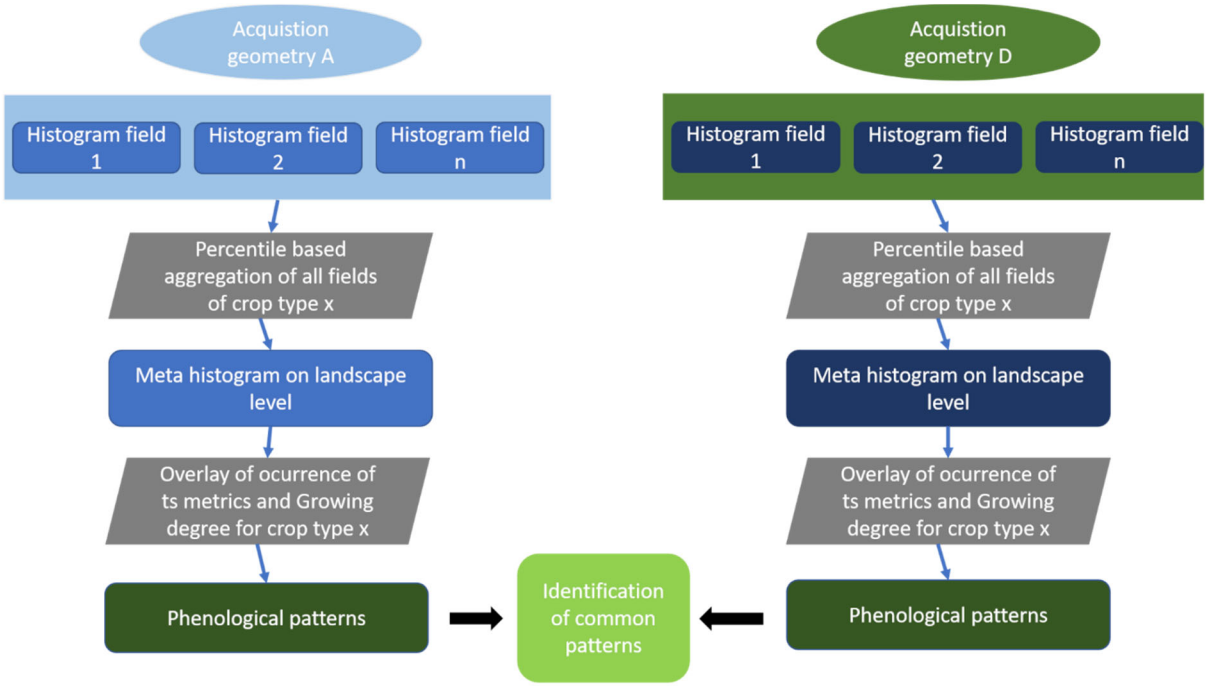

Fig 3: Generation of landscape level histogram for each Sentinel-1 feature containing the distribution pattern of relevant events within the time series for all fields of a specific crop identified by a threshold in number of occurrences

In a third step, an overlay is performed with the crop-specific GDD baseline, where significant occurrences of TSM are associated with specific ranges of GDD values.
This facilitates the allocation of phenological stages by matching them with the temporally closest phenological observation by DWD using differences in days and GDD (Day_observed – Day_tracked or GDD_observed – GDD_tracked). Executing this analysis in a multi-annual framework and for each relative orbit aims to uncover phenological events shaping crop-specific time series, providing insights into active and inactive periods within plant life cycles. It also reveals aspects of the plant life cycle not covered by the DWD monitoring framework, suggesting added value for Earth Observation-based phenological monitoring by filling data gaps.

3 Conclusion & Outlook

Since this contribtion's scope is limited, only the analysis output for wheat is shown as an exemplary exhibition of the extent of this analysis. All four investigated crop types have been investigated for relevant patterns of TSM at the landscape level. When looking at the exemplary patterns of wheat in Fig. 4, the following stages are highlighted.

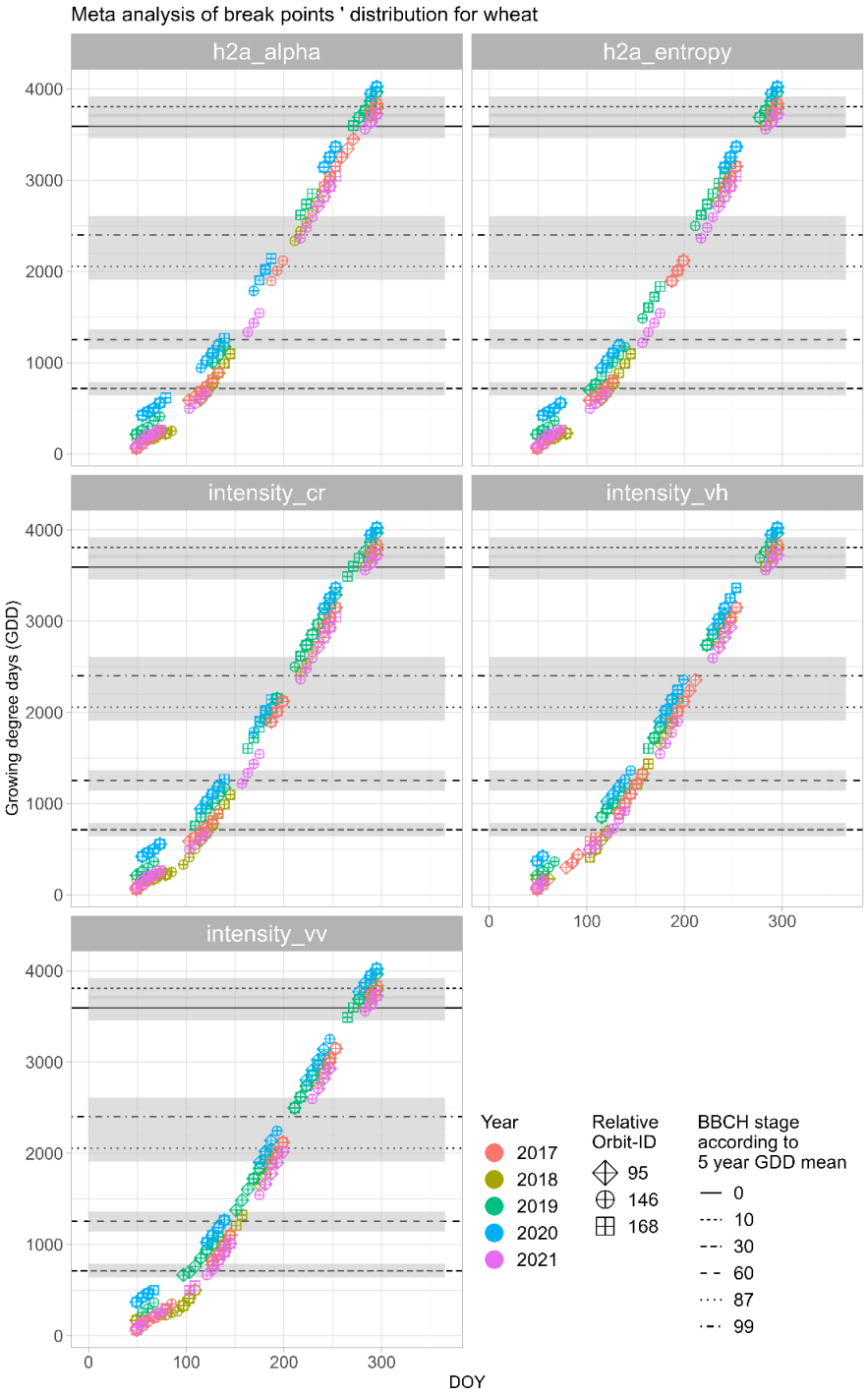

Fig 4: Distribution of relevant break points at the landscape level by orbit and year displaying patterns of increased occurrences in trend changes of the wheat specific time series. Being put in relation to Growing degree accumulation (GDD) and in situ observations of BBCH stages according to their 5-year GDD mean value and its standard deviation (grey areas)

ALP and ENT seem to pick up changes befor BBCH 30, around 250 GDD. Another major spot of trend changes is between BBCH 30 and 60 around 1000 GDD, hereby there is time shift related to years, where relative dry years of 2018, 2019 tend more towards BBCH 60 where as 2017 and 2021 are closer to BBCH 30. This shift is in line with stress related plant developments, where a plant shortens its vegetative period to conserve energy for its reproductive stage. The next conclusive accumulation of trend changes for ALP, ENT is between BBCH 99

and 0 which is related to the cultivation of intermediate crops such as mustard seed or clover. During this period ENT exhibits a less spread distribution, suggesting less sensitivity to developments of intermediary crops. At the end of the season (around DOY 300) both feature a break point accumulation. While BBCH 0 is covered by it it is more centered around BBCH 10 suggesting that Leaf development has a larger impact on the crop signature than cultivation.
The distributions of backscatter exhibit a similar behaviour, but one of the major differences is, that VV, VH and CR exhibit trend changes around 2000 GDD and BBCH 87. Furthermore, when comparing the compactness of distributions of ALP, ENT and VV, VH and CR by year and orbit ALP, ENT showcase less denser clusters, which suggest, that they are more sensitive to their respective viewing geometry. The analysis of maxima and minima revealed clusters in similar ranges of GDD values and around the same BBCH stages. Minima in ENT, ALP and CR signatures are linked to GDD values around 250 as well as the intermediary period; whereas VV and VH react to changes in plant structure at the onset of BBCH 60 between 1000 and 1250 GDD. When comparing the distribution of maxima to the minima's distribution across the season, ALP, ENT and CR change coverage with VV and VH. However, VV and VH are more sensitive towards plant changes around BBCH 87 and BBCH 99 as to changes in the intermediary stage. Furthermore, the distribution of minima appears far less concentrated, especially during the intermediary crop stage. This concurs with the following observation made during analysis: the occurrence and count of extrema is closely linked to the degree of smoothing.
The results of analysing potential systematic offsets related to viewing geometry, year and BBCH stage in break point occurrences are shown in Fig. 5. At first glance, the distributions of all features get more heterogenous with the increase in BBCH-value and no systematic shift by year or orbit is visible. Exceptions are made by ALP, ENT and CR in the year 2021 for the orbits 95 and 168 at BBCH 30 and VV at BBCH 87 and 99 for orbit 168 during the years 2018, 2020, 2021. As in the analysis shown above, CR, ALP and ENT display similar behaviour. Because VV displays the most compact smallest offsets measured in days, it is suggested that many crucial changes in wheat phenology are related to vertical plant elements susceptible to surface scattering (Löw et al. 2021). Also, the emergence of subsequent winter crops (BBCH 10) can be tracked with a small offset by all features. In regard to extreme value analysis, the patterns of the first step of analysis can be found. Relevant clusters of minima in VV and VH signatures are found close to BBCH 30 and 60, where at the stage of BBCH 30 a negative offset was observed. This negative offset is indicative for responsiveness towards developments that occur at later micro stages of BBCH 30 such as BBCH 33 or 35. A similar behaviour is reflected by maxima derived from signatures of ALP, ENT, and CR. Whereas maxima of VH signatures produce the best temporal match to BBCH 87. Additionally, this part of the analysis reveals another difference between extrema and break points. In the early stages of plant development (BBCH 0 to 30) extrema exhibit a greater sensitivity towards viewing geometry. Here tendencies to cluster by orbit and year can be detected. This indicates that after BBCH 30 the volume of biomass negates the effects of viewing geometry on forming crop specific signatures (Mercier et al. 2020).

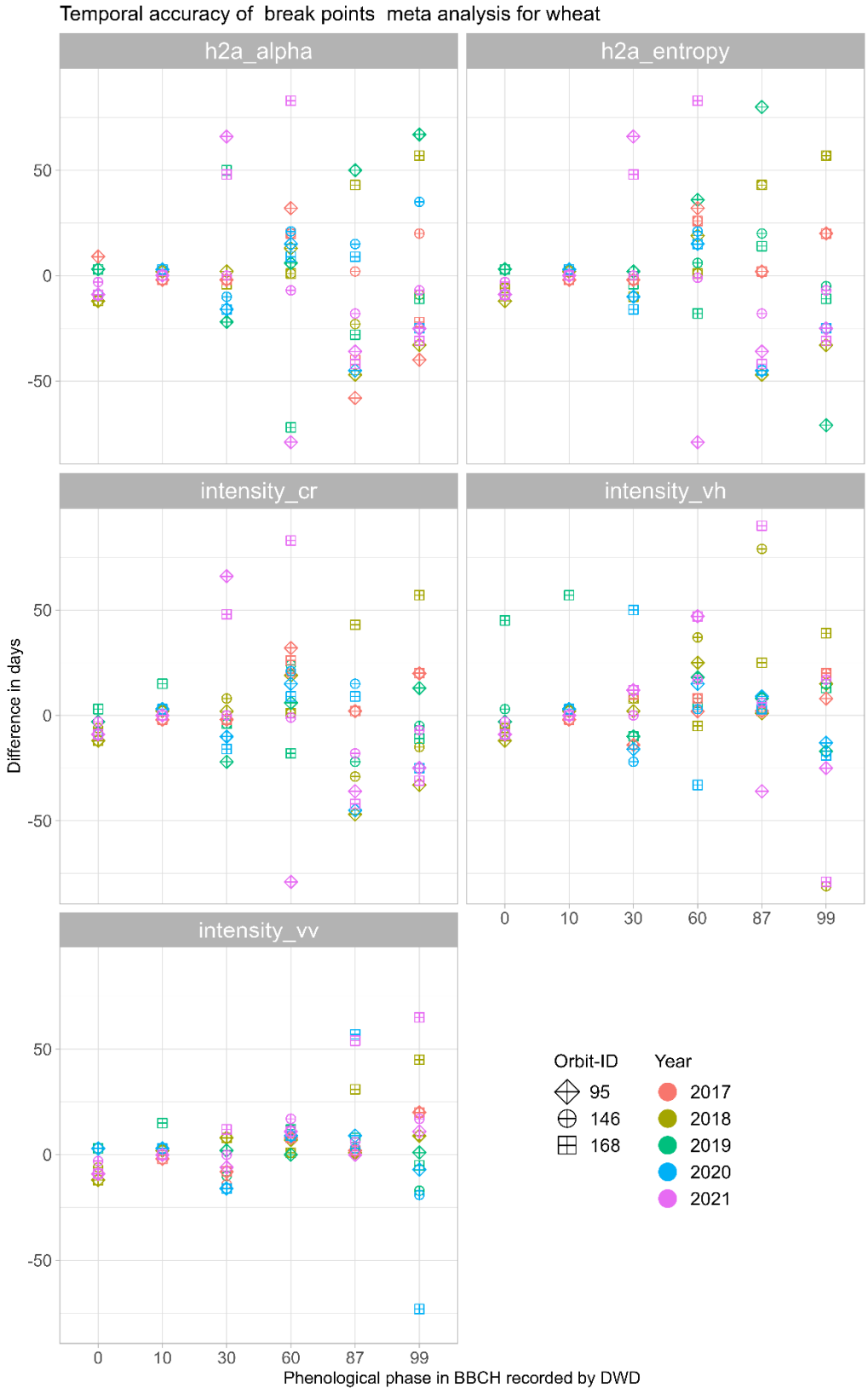

Fig 5: Temporal offset between relevant clusters of break points at landscape level and BBCH stages of wheat by year and relative orbit illustrating distribution patterns related to viewing geometries and years

The aggregated results of the previous part of the break point analysis are displayed as mean deviation by orbit, phenological stage and S1 feature alongside the variance of said deviation in Fig. 6. In an aggregated form the early stages of crop development (BBCH 0 and 10) exhibit an offset of around 10 days with a standard deviation of up to 6 days in all orbits and feature. Regarding BBCH 30, all features from orbit 168 as well as VV of all orbits and VH of orbit 95 display a negative offset of up to 10 days with a variance of below 10 days. Hence, in this stage of plant development features derived from orbit 146 and especially VV are most likely to yield - promising results for crop monitoring. Similar observations can be made for BBCH 60. However, the standard deviation of VV from all orbits is smaller than of any other feature. In this case the importance of viewing geometry is deemed irrelevant. BBCH 87 or yellow ripening also is best captured by VV. But here the results indicate that orbit 146 and 168 produce more stable results in break point allocation. BBCH 99 or harvesting is also most reliably tracked by VV or CR from orbit 146 and 168. However, by displaying a positive offset VV seems to track harvesting events earlier than CR. The investigation of minima showed that reliable tracking is only possible for BBCH 30 and 60 using VV and VH. Hereby, BBCH 30 is covered by orbits 146 and 168 for VV and orbit 95 and 146 for VH. Also, there is a negative offset of around 18-20 days, suggesting that minima pick up changes from a later micro stage of BBCH 30 such as BBCH 33 or 35. Flowering or BBCH 60 is more likely to be tracked by VV from orbit 168 and 146 as well as VH from orbit 95. As initially observed in the previous step, maxima in ALP, ENT and CR are deemed to reliably track BBCH 30 and 60 across all orbits. In the case of BBCH 30 an offset similar to the one of minima occurs. Changes around BBCH 87 are picked up by ALP, ENT, CR and VH across all orbits. VH exhibits the smallest offset, whereas ALP, ENT and CR show and increasingly positive offset and variance by orbit, indicating a sensitivity to viewing geometry. The offsets vary between 30 (orbit 168) to 47 (orbit 95) days. A similar pattern emerges at BBCH 99, but features from orbit 95 except for VV are not deemed reliable. The positive offsets in both phenological stadia can be interpreted in two ways. Either the phenological development of the focus region is around 20 to 40 day ahead of the average at federal state level or these features are more sensitive towards earlier changes during the ripening stages.

The same steps were conducted for the other crops: canola, sugar beet and potatoes. This provides and comparative and exhaustive overview of monitoring capabilities of S1 time series for a variety of crops. Furthermore, the analysis of relevant break point patterns uncovered stages of plant development for canola, potato and sugar beet which can be reliably tracked and are not covered by the DWD's statistics at federal state level. VV and VH signatures of canola produce a cluster at around 800-1000 GDD and DOY 175. Potatoes' signatures of all features, except VH produced a break point pattern of relevance at around 1200 GDD and DOY 200. Including VH a second pattern was found at around 1750 GDD and DOY 250. In regard to sugar beet, the additional pattern across all features was found at around 1500 GDD and DOY 200. Explaining the patterns of sugar beet and potato only by DWD observations proved to be difficult, because these two crops are among the less intensely monitored at federal state level. Only BBCH 0, 10 and 39 are covered by these statistics.

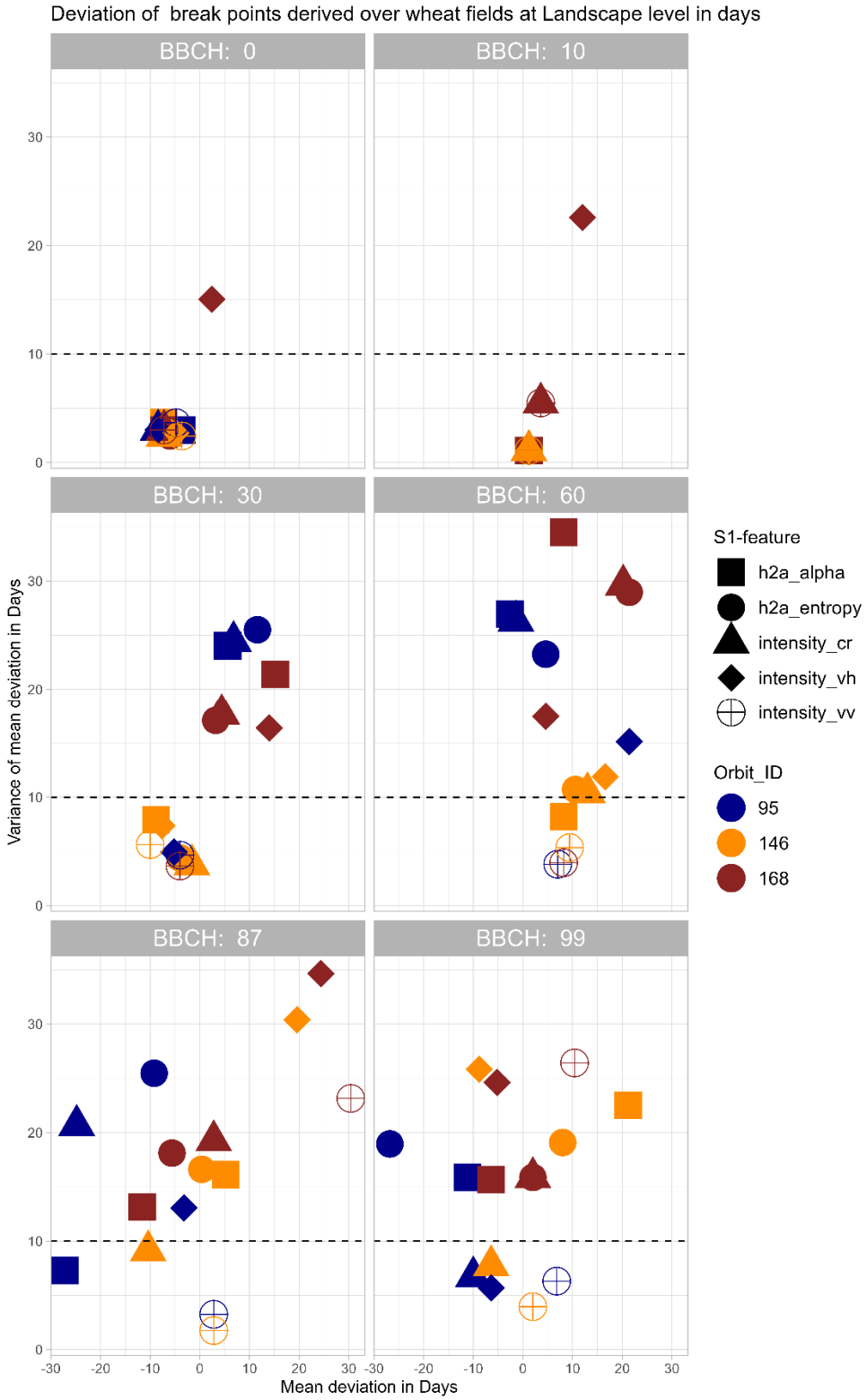

Fig 6.: Relevant occurrences of break points and their mean deviation by orbit, phenological stage and S1 feature alongside the variance of said deviation displaying their reliability in tracking certain BBCH stages (features below the dotted line)

In summary, this contribution presented a framework, that was able to capture and describe major parts of the inherent randomness (WOODHOUSE 2006) of SAR based time series derived over crop land. After analysing, the iteration of smoothing and its resulting distributions of

TSM it became apparent, that the selection and parametrization of the smoothing algorithm are an essential factor in evaluating TSM based results. This insight leads to the following conclusion: understanding and comparing results of studies presented by TSM focused work can only be done by rough estimates or educated guesses, if the selection and parametrization process of the smoothing algorithm is not transparent. Otherwise, the dimension of inaccuracy and information loss by introducing a smoothing algorithm cannot be assessed by the audience. In regard to employing extreme value analysis this study also reemphasizes the findings of MERONI et al. (2021), that a distinction between phenologically relevant and irrelevant extrema has to be made. Furthermore, it is concluded that extreme value analysis for SAR time series is best used, when there is a predetermined type sequence of extrema (e.g. max-min-max) that represents the targeted phenological developments.
In regard to future research, the next step would be to include InSAR coherence, which provides data on the temporal decorrelation during the plant life cycle, thus adding an additional source of information. Moreover, this examination of phenologically induced patterns using Sentinel-1 time series data at the landscape scale suggests two prospective avenues. Firstly, it facilitates the discernment of field-level dynamics within the broader landscape pattern, providing spatially explicit insights into a field's phenological progression relative to the overall trend. Anomalies in these patterns may indicate field-specific stressors such as lodging or pest infestations. Secondly, this research establishes a repository of documented phenological events associated with a growing degree baseline. Unlike purely retrospective records generated by break point and extreme value analyses, which encounter challenges in near-real-time applications, the satellite and GDD-based records in the archive can be harnessed for comparative scenario analyses. These analyses may evaluate the current season's performance by contrasting Sentinel-1 time series and GDD accumulation with previously tracked phenological developments in past seasons. Integration of weather forecasts can enhance this analysis, providing a forecasted outlook that estimates the ongoing season's phenological progress in comparison to recorded seasons, utilizing the projected GDD accumulation.

4 Literaturverzeichnis

ARIAS, M., CAMPO-BESCÓS, M.Á. & ÁLVAREZ-MOZOS, J., 2022: On the influence of acquisition geometry in backscatter time series over wheat. International Journal of Applied Earth Observation and Geoinformation, **106**, 102671, https://doi.org/10.1016/j.jag.2021.102671.

CANISIUS, F., SHANG, J., LIU, J., HUANG, X., MA, B., JIAO, X., GENG, X., KOVACS, J.M. & WALTERS, D., 2018: Tracking crop phenological development using multi-temporal polarimetric Radarsat-2 data. Remote Sens Environ, **210**, 508-518, https://doi.org/10.1016/j.rse.2017.07.031.

CLEVELAND, W.S., 1979: Robust Locally Weighted Regression and Smoothing Scatterplots Robust Locally Weighted Regression and Smoothing Scatterplots, **74**, 829-836, https://doi.org/10.2307/2286407.

CLOUDE, S.R. & POTTIER, E., 1996: A review of target decomposition theorems in radar polarimetry. IEEE Transactions on Geoscience and Remote Sensing, 34, 498-518, https://doi.org/10.1109/36.485127.

DERAKHSHAN, A., BAKHSHANDEH, A., SIADAT, S.A. ALLAH, MORADI-TELAVAT, M.R. & ANDARZIAN, S.B., 2018: Quantifying the germination response of spring canola (Brassica napus L.) to temperature. Ind Crops Prod, **122**, 195-201, https://doi.org/10.1016/j.indcrop.2018.05.075.

GAO, F. & ZHANG, X., 2021: Mapping Crop Phenology in Near Real-Time Using Satellite Remote Sensing: Challenges and Opportunities. Journal of Remote Sensing, https://doi.org/10.34133/2021/8379391.

GILLIAMS, S., WHITCRAFT, A., KOMMAREDDY, I., HAYNES, K. & JARVIS, I., n.d. EAV Home | AgVariables [WWW Document]. https://agvariables.org/ last access 29.11.23.

HARFENMEISTER, K., ITZEROTT, S., WELTZIEN, C. & SPENGLER, D., 2021: Agricultural Monitoring Using Polarimetric Decomposition Parameters of Sentinel-1 Data. Remote Sensing, **13**, 575, https://doi.org/10.3390/rs13040575.

HAßELBUSCH, K. & LUCAS-MOFAT, A., 2021: Rasterdaten für die Agrarmeteorologie: Vergleich verschiedener Interpolationsverfahren am Beispiel AgriSens Demmin 4.0. Braunschweig.

HAVERKORT, A.J. & VERHAGEN, A., 2008: Climate change and its repercussions for the potato supply chain. Potato Research. Springer, 223-237, https://doi.org/10.1007/s11540-008-9107-0.

JACOTT, C.N. & BODEN, S.A., 2020: Feeling the heat: Developmental and molecular responses of wheat and barley to high ambient temperatures. J Exp Bot, https://doi.org/10.1093/jxb/eraa326.

KHABBAZAN, S., VERMUNT, P., STEELE-DUNNE, S., ARNTZ, L.R., MARINETTI, C., VAN DER VALK, D., IANNINI, L., MOLIJN, R., WESTERDIJK, K. & VAN DER SANDE, C., 2019: Crop monitoring using Sentinel-1 data: A case study from The Netherlands. Remote Sensing, **11**, 1-24, https://doi.org/10.3390/rs11161887.

LOBERT, F., LÖW, J., SCHWIEDER, M., GOCHT, A., SCHLUND, M., HOSTERT, P. & ERASMI, S., 2023: A deep learning approach for deriving winter wheat phenology from optical and SAR time series at field level. Remote Sens Environ, **298**, 113800, https://doi.org/10.1016/j.rse.2023.113800.

LÖW, J., ULLMANN, T. & CONRAD, C., 2021: The impact of phenological developments on interferometric and polarimetric crop signatures derived from sentinel-1: Examples from the DEMMIN study site (Germany). Remote Sensing, **13**, https://doi.org/10.3390/rs13152951.

MCMASTER, G.S.& SMIKA, D.E., 1988: Estimation and evaluation of winter wheat phenology in the central Great Plains. Agric For Meteorol, **43**, 1-18, https://doi.org/10.1016/0168-1923(88)90002-0.

MCMASTER, G.S. & WILHELM, W.W., 1997: Growing degree-days: One equation, two interpretations. Agric For Meteorol, **87**, 291-300, https://doi.org/10.1016/S0168-1923(97)00027-0.

MCNAIRN, H., JIAO, X., PACHECO, A., SINHA, A., TAN, W. & LI, Y., 2018: Estimating canola phenology using synthetic aperture radar. Remote Sens Environ, **219**, 196-205, https://doi.org/10.1016/j.rse.2018.10.012.

MERCIER, A., BETBEDER, J., BAUDRY, J., LE ROUX, V., SPICHER, F., LACOUX, J., ROGER, D. & HUBERT-MOY, L., 2020: Evaluation of Sentinel-1 & 2 time series for predicting wheat and rapeseed phenological stages. ISPRS Journal of Photogrammetry and Remote Sensing, **163**, 231-256, https://doi.org/10.1016/j.isprsjprs.2020.03.009.

NASRALLAH, A., BAGHDADI, N., EL HAJJ, M., DARWISH, T., BELHOUCHETTE, H., FAOUR, G., DARWICH, S. & MHAWEJ, M., 2019: Sentinel-1 Data for Winter Wheat Phenology Monitoring and Mapping. Remote Sensing, **11**, 2228, https://doi.org/10.3390/rs11192228.

PASTERNAK, M. & PAWŁUSZEK-FILIPIAK, K., 2023: Evaluation of C and X-Band Synthetic Aperture Radar Derivatives for Tracking Crop Phenological Development. Remote Sensing, **15**, 4996, https://doi.org/10.3390/RS15204996.

QADIR, A., SKAKUN, S., EUN, J., PRASHNANI, M. & SHUMILO, L., 2023: Sentinel-1 time series data for sunflower (Helianthus annuus) phenology monitoring. Remote Sens Environ, **295**, 113689, https://doi.org/10.1016/j.rse.2023.113689.

RADKE, J.K. & BAUER, R.E., 1969: Growth of Sugar Beets as Affected by Root Temperatures Part I: Greenhouse Studies[1]. Agronomy Journal, **61**(6), 860-863, https://doi.org/10.2134/agronj1969.00021962006100060009x.

REYERS, B., STAFFORD-SMITH, M., ERB, K.H., SCHOLES, R.J. & SELOMANE, O., 2017: Essential Variables help to focus Sustainable Development Goals monitoring. Curr Opin Environ Sustain. https://doi.org/10.1016/j.cosust.2017.05.003.

RITCHIE, J.T. & NESMITH, D.S., 2015: Temperature and crop development, in: Modeling Plant and Soil Systems. Wiley Blackwell, 5-29. https://doi.org/10.2134/agronmonogr31.c2.

RYKACZEWSKA, K., 2015: The Effect of High Temperature Occurring in Subsequent Stages of Plant Development on Potato Yield and Tuber Physiological Defects. American Journal of Potato Research, **92**, 339-349, https://doi.org/10.1007/s12230-015-9436-x.

SAKAMOTO, T., GITELSON, A.A. & ARKEBAUER, T.J., 2013: MODIS-based corn grain yield estimation model incorporating crop phenology information. Remote Sens Environ, **131**, 215-231, https://doi.org/https://doi.org/10.1016/j.rse.2012.12.017.

SCHLUND, M. & ERASMI, S., 2020: Sentinel-1 time series data for monitoring the phenology of winter wheat. Remote Sens Environ, **246**, 111814, https://doi.org/10.1016/j.rse.2020.111814.

SHORACHI, M., KUMAR, V. & STEELE-DUNNE, S.C., 2022: Sentinel-1 SAR Backscatter Response to Agricultural Drought in The Netherlands. Remote Sensing, **14**, 2435, https://doi.org/10.3390/rs14102435.

SPENGLER, D., ITZEROTT, S., AHMADIAN, N., BORG, E., HÜTTICH, C., MAASS, H., MISSLING, K.-D., SCHMULLIUS, C., TRUCKENBRODT, S. & CONRAD, C., 2018: The German JECAM site DEMMIN: status and future perspectives. Annual JECAM Meeting. Taichung City, Taiwan.

STEELE-DUNNE et al., SC., 2017: Radar Remote Sensing of Agriciltural Canopies. IEEE J. Sel. Top. Appl. Earth Obs. Rem. Sen, **10**, 2249-2273.

STINNER, R.E., GUTIERREZ, A.P. & BUTLER, G.D., 1974: An algorithm for temperature-dependent growth rate simulation. Can Entomol, **106**, 519-524, https://doi.org/10.4039/Ent106519-5.

TERRY, N., 1968: Developmental Physiology of Sugar Beet: I. The Influence of Light and Temperature on Growth. J Exp Bot, **19**, 795-811.

TRUCKENBRODT, J., CREMER, F. & EBERLE, J., 2019: pyroSAR-A Framework for Large-Scale SAR Satellite Data Processing. ESA Living Planet Symposium, Milan, Italy. https://doi.org/10.13140/RG.2.2.16424.83206.

VERBESSELT, J., HYNDMAN, R., ZEILEIS, A. & CULVENOR, D., 2010: Phenological change detection while accounting for abrupt and gradual trends in satellite image time series. Remote Sens Environ, **114**, 2970-2980, https://doi.org/https://doi.org/10.1016/j.rse.2010.08.003.

VERBESSELT, J., ZEILEIS, A. & HEROLD, M., 2012: Near real-time disturbance detection using satellite image time series. Remote Sens Environ, **123**, 98-108, https://doi.org/https://doi.org/10.1016/j.rse.2012.02.022.

VREUGDENHIL, M., WAGNER, W., BAUER-MARSCHALLINGER, B., PFEIL, I., TEUBNER, I., RÜDIGER, C. & STRAUSS, P., 2018: Sensitivity of Sentinel-1 backscatter to vegetation dynamics: An Austrian case study. Remote Sensing, **10**, 1-19, https://doi.org/10.3390/rs10091396.

WOODHOUSE, I.H., 2006: Introduction to Microwave Remote Sensing. CRC Press, Boca Raton.

ZHOU, G. & Wang, Q., 2018: A new nonlinear method for calculating growing degree days. Sci Rep, **8**, 1-14, https://doi.org/10.1038/s41598-018-28392-z.